Measurement of the CP-Violating Phase phi(s) in (B)over-bar(s)(0) -> Ds+Ds- Decays

Aaij, R.; Abellan Beteta, C.; Adeva, B.; Adinolfi, M.; Affolder, A.; Ajaltouni, Z.; Akar, S.; Albrecht, J.; Alessio, F.; Alexander, M.

IMPORTANT NOTE: You are advised to consult the publisher's version (publisher's PDF) if you wish to cite from it. Please check the document version below.

Document Version
Publisher's PDF, also known as Version of record

Publication date:
2014

Link to publication in University of Groningen/UMCG research database

PHYSICAL REVIEW LETTERS

Measurement of the *CP*-Violating Phase ϕ_s in $\bar{B}_s^0 \to D_s^+ D_s^-$ Decays

R. Aaij *et al.*[*]

(LHCb Collaboration)

We present a measurement of the *CP*-violating weak mixing phase ϕ_s using the decay $\bar{B}_s^0 \to D_s^+ D_s^-$ in a data sample corresponding to $3.0\,\text{fb}^{-1}$ of integrated luminosity collected with the LHCb detector in pp collisions at center-of-mass energies of 7 and 8 TeV. An analysis of the time evolution of the system, which does not use the constraint $|\lambda| = 1$ to allow for the presence of *CP* violation in decay, yields $\phi_s = 0.02 \pm 0.17(\text{stat}) \pm 0.02(\text{syst})$ rad, $|\lambda| = 0.91^{+0.18}_{-0.15}(\text{stat}) \pm 0.02(\text{syst})$. This result is consistent with the standard model expectation.

The *CP*-violating weak mixing phase ϕ_s can be measured in the interference between mixing and decay of $\bar{B}_s^0$ mesons to *CP* eigenstates that proceeds via the $b \to c\bar{c}s$ transition and is predicted to be small in the standard model (SM): $\phi_s^{\text{SM}} \approx -2\beta_s \equiv -2\arg[-(V_{ts}V_{tb}^*)/(V_{cs}V_{cb}^*)] = -36.3^{+1.6}_{-1.5}$ mrad [1]. Measurements of ϕ_s are sensitive to the effects of potential non-SM particles contributing to the B_s^0-$\bar{B}_s^0$ mixing amplitude. Several measurements of ϕ_s have been made with the decay mode $\bar{B}_s^0 \to J/\psi\phi$, with the first results showing tension with the SM expectation [2,3]. Since then, more recent measurements of ϕ_s have found values consistent with the SM prediction in $\bar{B}_s^0 \to J/\psi K^+ K^-$ and $\bar{B}_s^0 \to J/\psi \pi^+ \pi^-$ decays [4–8]. The world average value determined prior to the publication of Ref. [5] is $\phi_s = 0 \pm 70$ mrad [9].

Precise measurements of ϕ_s are complicated by the presence of loop (penguin) diagrams, which could have an appreciable effect [10]. It is, therefore, important to measure ϕ_s in additional decay modes where penguin amplitudes may differ [11]. Additionally, in the $\bar{B}_s^0 \to J/\psi\phi$ channel, where a spin-0 meson decays to two spin-1 mesons, an angular analysis is required to disentangle statistically the *CP*-even and *CP*-odd components. The decay $\bar{B}_s^0 \to D_s^+ D_s^-$ is also a $b \to c\bar{c}s$ transition with which ϕ_s can be measured [12], with the advantage that the $D_s^+ D_s^-$ final state is *CP* even and does not require angular analysis.

In this Letter, we present the first measurement of ϕ_s in $\bar{B}_s^0 \to D_s^+ D_s^-$ decays using an integrated luminosity of $3.0\,\text{fb}^{-1}$, obtained from pp collisions collected by the LHCb detector. One third of the data were collected at a center-of-mass energy of 7 TeV and the remainder at 8 TeV.

We perform a fit to the time evolution of the $\bar{B}_s^0$-B_s^0 system in order to extract ϕ_s.

LHCb is a single-arm forward spectrometer at the LHC designed for the study of particles containing b or c quarks in the pseudorapidity range of 2 to 5 [13]. Events are selected by a trigger consisting of a hardware stage that identifies high transverse energy particles, followed by a software stage, which applies a full event reconstruction [14]. A multivariate algorithm [15] is used to select candidates with secondary vertices consistent with the decay of a b hadron.

Signal $\bar{B}_s^0 \to D_s^+ D_s^-$ candidates are reconstructed in four final states: (i) $D_s^+ \to K^+ K^- \pi^+, D_s^- \to K^- K^+ \pi^-$; (ii) $D_s^+ \to K^+ K^- \pi^+, D_s^- \to \pi^- \pi^+ \pi^-$; (iii) $D_s^+ \to K^+ K^- \pi^+, D_s^- \to K^- \pi^+ \pi^-$; and (iv) $D_s^+ \to \pi^+ \pi^- \pi^+, D_s^- \to \pi^- \pi^+ \pi^-$. The inclusion of charge-conjugate processes, unless otherwise specified, is implicit. The $B^0 \to D^- D_s^+$ decay mode, where $D^- \to K^+ \pi^- \pi^-$ and $D_s^+ \to K^+ K^- \pi^+$, is used as a control channel. The selection requirements follow Ref. [16], apart from minor differences in the particle identification requirements and $B_{(s)}$ candidate mass regions. $D_{(s)}$ meson candidates are required to have masses within 25 MeV/c^2 of their known values [17] and to have a significant separation from the $B_{(s)}$ vertex. As the signatures of b-hadron decays to double-charm final states are all similar, vetoes are employed to suppress the cross feed resulting from particle misidentification, following Ref. [18]. All $B_{(s)}$ candidates are refitted, taking both $D_{(s)}$ mass and vertex constraints into account [19]. A boosted decision tree (BDT) [20,21] is used to improve the signal to background ratio. The BDT is trained with simulated decays to emulate the signal and same-charge $D_s^+ D_s^+$ and $D^+ D_s^+$ from candidates with masses in the range $5200 < M(D_s^+ D_s^+) < 5650$ MeV/c^2 and $5200 < M(D^+ D_s^+) < 5600$ MeV/c^2, respectively. The selection requirement on the BDT output, which retains about 98% of the signal events, is chosen to minimize the expected relative uncertainty in the $\bar{B}_s^0 \to D_s^+ D_s^-$ yield. The $B_{(s)}$ candidates are required to lie in the mass regions
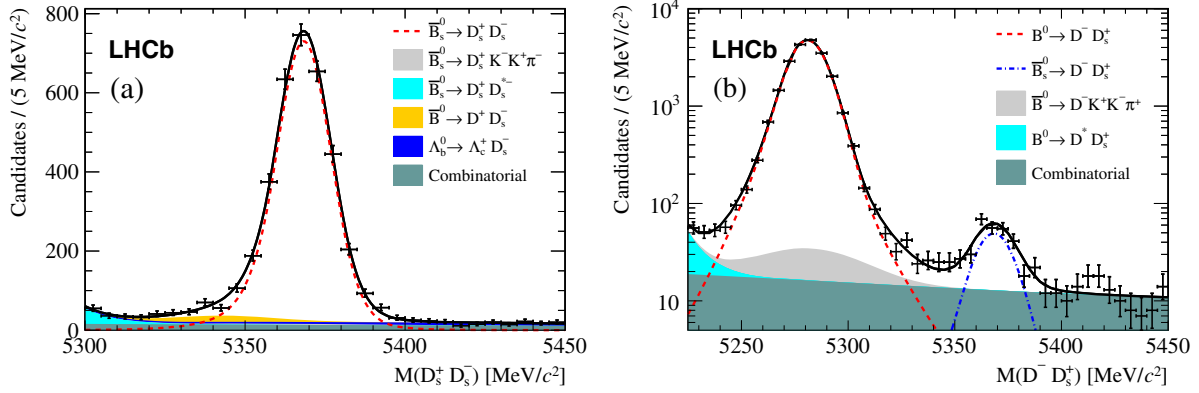
[*]Full author list given at the end of the article.

FIG. 1 (color online).   Invariant mass distributions of (a) $\bar{B}_s^0 \to D_s^+ D_s^-$ and (b) $B^0 \to D^- D_s^+$ candidates. The points show the data; the individual fit components are indicated in the legend; the black curve shows the overall fit.

$5300 < M(D_s^+ D_s^-) < 5450$ MeV/c^2 for the signal and $5200 < M(D^- D_s^+) < 5450$ MeV/c^2 for the control channel, where the lower bound is chosen to suppress background contributions from $B_{(s)}$ decays with excited charm mesons in the final state. The decay time distribution is fitted in the range $0.2 < t < 12.0$ ps where the lower bound is chosen to reduce backgrounds from particles originating from the primary vertex.

The mass distributions for the signal, summed over the four final states, and the control channel are shown in Fig. 1, with results of unbinned maximum likelihood fits overlaid. The signal shapes are parametrized by the sum of two asymmetric Gaussian functions with a common mean. The background shapes are obtained from simulation [22–25]. Background rates from misidentified particles are obtained from $D^{*+} \to D^0 \pi^+$, $D^0 \to K^- \pi^+$ calibration data. Signal and background components are described in Ref. [16]. All yields in the fits to the full data sample are allowed to vary, except that corresponding to $\bar{B}_{(s)}^0 \to D_{(s)}^+ K^- K^+ \pi^-$ decays, which is fixed to be 1% of the signal yield as determined from a fit to the D_s mass sidebands. We observe 3345 ± 62 $\bar{B}_s^0 \to D_s^+ D_s^-$ signal and 21320 ± 148 $B^0 \to D^- D_s^+$ control channel decays. In the $D^- D_s^+$ channel, we also observe a contribution from $\bar{B}_s^0 \to D_s^+ D^-$ as reported previously [18]. We use the *sPlot* technique [26] to obtain the decay time distribution of $\bar{B}_s^0 \to D_s^+ D_s^-$ signal decays where the $D_s^+ D_s^-$ invariant mass is the discriminating variable. A fit to the background-subtracted distribution of the decay time t is performed using the signal-only decay time probability density function (PDF). The negative log likelihood to be minimized is

$$-\ln \mathcal{L} = -\alpha \sum_i^N W_i \ln \mathcal{P}(t_i, \delta_i, q_i^{\text{tag}} | \eta_i^{\text{tag}}), \quad (1)$$

where N denotes the total number of signal and background candidates in the fit region, W_i is the signal component weight, and $\alpha = \sum_i^N W_i / \sum_i^N W_i^2$ [27]. The invariant mass is not correlated with the reconstructed decay time or its

uncertainty, nor with flavor tagging output, for signal and background. The signal PDF $\mathcal{P}$ includes detector resolution and acceptance effects and requires knowledge of the $B_s^0(\bar{B}_s^0)$ flavor at production,

$$\mathcal{P}(t, \delta, q^{\text{tag}} | \eta^{\text{tag}}) = R(\hat{t}, q^{\text{tag}} | \eta^{\text{tag}}) \otimes G(t - \hat{t} | \delta) \times \epsilon_{\text{data}}^{D_s^+ D_s^-}(t), \quad (2)$$

where $\hat{t}$ is the decay time in the absence of resolution effects, $R(\hat{t}, q^{\text{tag}} | \eta^{\text{tag}})$ describes the rate including imperfect knowledge of the initial $\overset{(-)0}{B}{}_s$ flavor through the flavor tag q^{tag}, and the wrong-tag probability estimate η^{tag}. The flavor tag q^{tag} is -1 for $\bar{B}_s^0$, $+1$ for B_s^0, and zero for untagged candidates. The calibrated decay time resolution is $G(t - \hat{t} | \delta)$ where δ is the decay time error estimate and $\epsilon_{\text{data}}^{D_s^+ D_s^-}(t)$ is the decay time acceptance.

Allowing for *CP* violation in decay, the decay rates of $\overset{(-)0}{B}{}_s$ mesons ignoring detector effects can be written as

$$\Gamma(\hat{t}) = \mathcal{N} e^{-\Gamma_s \hat{t}} \left[\cosh\left(\frac{\Delta\Gamma_s}{2}\hat{t}\right) - \frac{2|\lambda|\cos\phi_s}{1+|\lambda|^2}\sinh\left(\frac{\Delta\Gamma_s}{2}\hat{t}\right) \right.$$
$$\left. + \frac{1-|\lambda|^2}{1+|\lambda|^2}\cos(\Delta m_s \hat{t}) - \frac{2|\lambda|\sin\phi_s}{1+|\lambda|^2}\sin(\Delta m_s \hat{t}) \right], \quad (3)$$

$$\bar{\Gamma}(\hat{t}) = \left|\frac{p}{q}\right|^2 \mathcal{N} e^{-\Gamma_s \hat{t}} \left[\cosh\left(\frac{\Delta\Gamma_s}{2}\hat{t}\right) - \frac{2|\lambda|\cos\phi_s}{1+|\lambda|^2}\sinh\left(\frac{\Delta\Gamma_s}{2}\hat{t}\right) \right.$$
$$\left. - \frac{1-|\lambda|^2}{1+|\lambda|^2}\cos(\Delta m_s \hat{t}) + \frac{2|\lambda|\sin\phi_s}{1+|\lambda|^2}\sin(\Delta m_s \hat{t}) \right], \quad (4)$$

where $\Gamma_s \equiv (\Gamma_L + \Gamma_H)/2$ is the average decay width of the light and heavy mass eigenstates, $\Delta\Gamma_s \equiv \Gamma_L - \Gamma_H$ is their decay width difference, and $\Delta m_s \equiv m_H - m_L$ is their mass difference. As Δm_s is large [28] and the production asymmetry is small [29], the effect of the production asymmetry is negligible, and so the constant $\mathcal{N}$ is the same for both B_s^0 and $\bar{B}_s^0$ mesons. Similarly, we do not

consider a tagging asymmetry in the fit as this is known to be consistent with zero. CP violation in mixing and decay is parametrized by the factor $\lambda \equiv (q/p)(\bar{A}_f/A_f)$, with $\phi_s \equiv -\arg(\lambda)$. The terms A_f ($\bar{A}_f$) are the amplitudes for the B_s^0 ($\bar{B}_s^0$) decay to the final state f, which in this case is $f = D_s^+ D_s^-$, and the complex parameters $p = \langle B_s^0 | B_L \rangle$ and $q = \langle \bar{B}_s^0 | B_L \rangle$ relate the mass and flavor eigenstates. The factor $|p/q|^2$ in Eq. (4) is related to the flavor-specific CP asymmetry $a_{\rm sl}^s$ by

$$a_{\rm sl}^s = \frac{|p/q|^2 - |q/p|^2}{|p/q|^2 + |q/p|^2} \approx |p/q|^2 - 1. \qquad (5)$$

LHCb has measured $a_{\rm sl}^s = [-0.06 \pm 0.50(\text{stat}) \pm 0.36(\text{syst})]\%$ [30], implying $|p/q|^2 = 0.9994 \pm 0.0062$. We assume that it is unity in this analysis and that any observed deviation of $|\lambda|$ from 1 is due to CP violation in the decay, i.e., $|\bar{A}_f/A_f| \neq 1$.

The initial flavor of the signal b hadron is determined using two methods. In hadron collisions, b hadrons are mostly produced as pairs: the opposite-side (OS) tagger [31] determines the flavor of the other b hadron in the event by identifying the charges of the leptons and kaons into which it decays, or the net charge of particles forming a detached vertex consistent with that of a b hadron. The neural network same-side (SS) kaon tagger [4] exploits the hadronization process in which the fragmentation of a $\bar{b}(b)$ into a $B_s^0(\bar{B}_s^0)$ meson leads to an extra $\bar{s}(s)$ quark, which often forms a $K^+(K^-)$ meson, the charge of which identifies the initial $\overset{(-)}{B}{}_s^0$ flavor. The SS kaon tagger uses an improved algorithm with respect to Ref. [4] that enhances the fraction of correctly tagged mesons by 40%. In both tagging algorithms, a per-event wrong-tag probability estimate $\eta^{\rm tag}$ is determined based on the output of a neural network trained on either simulated $\bar{B}_s^0 \to D_s^+ \pi^-$ events for the SS tagger or, in the case of the OS algorithm, using a data sample of $B^- \to J/\psi K^-$ decays. The taggers are then calibrated in data using flavor-specific decay modes in order to provide a per-event wrong-tag probability $\overset{(-)}{\omega}(\eta^{\rm tag})$ for an initial flavor $\overset{(-)}{B}{}_s^0$ meson. The calibration is performed separately for the two tagging algorithms, which are then combined in the fit. The effective tagging power is parametrized by $\varepsilon_{\rm tag} D^2$ where $D \equiv (1 - 2\omega)$ and $\varepsilon_{\rm tag}$ is the fraction of events tagged by the algorithm.

The combined effective tagging power is $\varepsilon_{\rm tag} D^2 = [5.33 \pm 0.18(\text{stat}) \pm 0.17(\text{syst})]\%$, comparable to that of other recent analyses [32]. The rate expression including flavor tagging is

$$\begin{aligned} R(\hat{t}, &q^{\rm OS}|\eta^{\rm OS}, q^{\rm SS}|\eta^{\rm SS}) \\ &= (1 + q^{\rm OS}[1 - 2\omega^{\rm OS}])(1 + q^{\rm SS}[1 - 2\omega^{\rm SS}])\Gamma(\hat{t}) \\ &+ (1 - q^{\rm OS}[1 - 2\bar{\omega}^{\rm OS}])(1 - q^{\rm SS}[1 - 2\bar{\omega}^{\rm SS}])\bar{\Gamma}(\hat{t}). \end{aligned} \quad (6)$$

The track reconstruction, trigger, and selection efficiencies vary as a function of decay time, requiring that an acceptance function is included in the fit. The $\bar{B}_s^0 \to D_s^+ D_s^-$ acceptance is determined using

$$\varepsilon_{\rm data}^{D_s^+ D_s^-}(t) = \varepsilon_{\rm data}^{D^- D_s^+}(t) \times \frac{\varepsilon_{\rm sim}^{D_s^+ D_s^-}}{\varepsilon_{\rm sim}^{D^- D_s^+}}(t), \qquad (7)$$

where $\varepsilon_{\rm data}^{D^- D_s^+}(t)$ is the efficiency associated with the $B^0 \to D^- D_s^+$ control channel as determined directly from the data and $\varepsilon_{\rm sim}^{D_s^+ D_s^-}/\varepsilon_{\rm sim}^{D^- D_s^+}(t)$ is the relative efficiency obtained from simulation after all selections are applied. This correction accounts for the differences in lifetime as well as small kinematic differences between the signal and control channels. The first factor in Eq. (7) is

$$\varepsilon_{\rm data}^{D^- D_s^+}(t) = \frac{N_{\rm data}^{D^- D_s^+}(t)}{\mathcal{N} e^{-\Gamma_d \hat{t}} \otimes G(t - \hat{t}|\sigma_{\rm eff})}, \qquad (8)$$

where $N_{\rm data}^{D^- D_s^+}(t)$ denotes the number of $B^0 \to D^- D_s^+$ signal decays in a given bin of the decay time distribution, $\mathcal{N} e^{-\Gamma_d \hat{t}}$ is an exponential with decay width equal to that of the world average value for B^0 mesons [17], $\mathcal{N}$ is a constant, and $G(t - \hat{t}|\sigma_{\rm eff})$ is a Gaussian resolution function with width $\sigma_{\rm eff} = 54$ fs, determined from simulation. In the fit, the acceptance is implemented as a histogram. The binning scheme is chosen to maintain approximately equal statistical power in each bin. Figure 2(a) shows $\varepsilon_{\rm data}^{D^- D_s^+}(t)$ and $\varepsilon_{\rm sim}^{D^- D_s^+}(t)$, while Fig. 2(b) shows $\varepsilon_{\rm sim}^{D_s^+ D_s^-}(t)$ and $\varepsilon_{\rm data}^{D_s^+ D_s^-}(t)$ as used in the fit to extract ϕ_s. The procedure is verified by fitting for the decay width in both the signal and the control channels, where the results are found to be consistent with the published values.

The fit to determine ϕ_s uses a decay time uncertainty estimated in each event and obtained from the constrained vertex fit from which the decay time is determined. The resolution function is

$$G(t - \hat{t}|\delta) = \frac{1}{\sqrt{2\pi}\sigma(\delta)} e^{-\frac{1}{2}\left(\frac{t - \hat{t}}{\sigma(\delta)}\right)^2}. \qquad (9)$$

The per-event resolution $\sigma(\delta)$ is calibrated using simulated signal decays by fitting the effective resolution $\sigma_{\rm eff}$ in bins of the per-event decay time error estimate $\sigma_{\rm eff} = q_0 + q_1 \delta$. The effective resolution is determined by fitting to the event-by-event decay time difference between the reconstructed and generated decay time in simulated signal decays. The effective resolution is the sum in quadrature of the widths of two Gaussian functions contributing with their corresponding fractions. The values $q_0 = 8.9 \pm 1.3$ fs and $q_1 = 1.014 \pm 0.036$ are obtained from the fit, resulting in a calibrated effective resolution of 54 fs.

In the fits that determine ϕ_s, we apply Gaussian constraints to the average decay width $\Gamma_s = 0.661 \pm 0.007 \, \text{ps}^{-1}$, the decay width difference $\Delta\Gamma_s = 0.106 \pm 0.013 \, \text{ps}^{-1}$ [4],
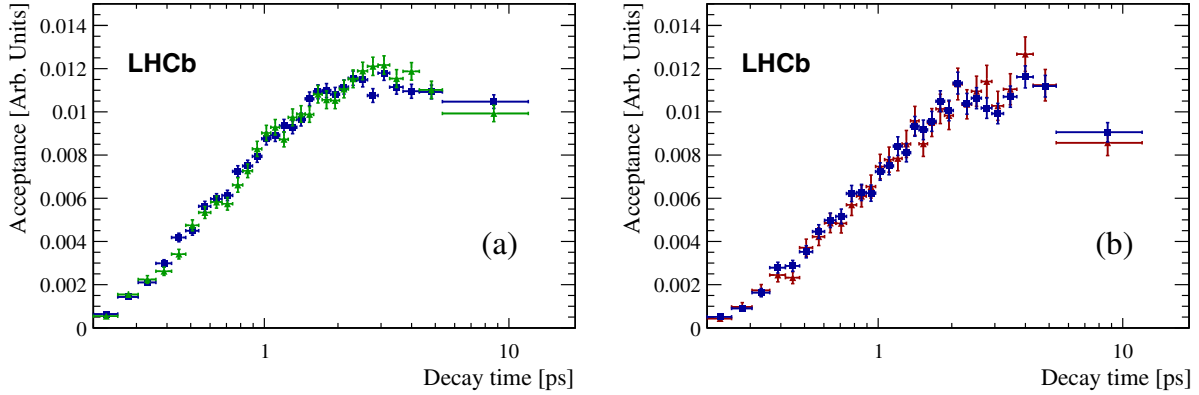
FIG. 2 (color online).   Decay time acceptances in simulation and data. (a) $B^0 \to D^- D_s^+$ acceptance in data (green triangles) and simulation (blue squares). (b) $\bar{B}_s^0 \to D_s^+ D_s^-$ acceptance in simulation (blue squares) and the $B^0 \to D^- D_s^+$ acceptance corrected for $\bar{B}_s^0 \to D_s^+ D_s^-$ (red triangles). The correction is described in detail in the text.

the mixing frequency $\Delta m_s = 17.168 \pm 0.024$ ps^{-1} [28], and the flavor tagging and resolution calibration parameters. The correlation between Γ_s and $\Delta\Gamma_s$ is accounted for in the fit. Two fits to the data are performed, one assuming no CP violation in decay, i.e., $|\lambda| = 1$, and a second where this assumption is removed. The fit is validated using pseudoexperiments and simulated LHCb events.

The systematic uncertainties on ϕ_s and $|\lambda|$ that are not accounted for by the use of Gaussian constraints are summarized in Table I. The systematic uncertainty associated with the resolution calibration in simulated events is studied by generating pseudoexperiments with an alternative resolution parameterization ($q_0 = 0$, $q_1 \in [1.25, 1.45]$ [28]) obtained in $\bar{B}_s^0$ decays in data. The effect of mismodeling of the mass PDF is studied by fitting using a larger mass window and including an additional background component from $\bar{B}_s^0 \to D_s^{*+} D_s^{*-}$. The effect of mismodeling the acceptance distribution is studied by fitting the $\bar{B}_s^0 \to D_s^+ D^-$ derived acceptance in pseudoexperiments generated with the acceptance distribution determined entirely from $\bar{B}_s^0 \to D_s^+ D_s^-$ simulation. The uncertainty due to the finite size of the simulated data samples used to determine the acceptance correction is evaluated by fitting to the data 500 times with Gaussian fluctuations around the bin values with a width equal to the statistical uncertainties. We evaluate the uncertainty due to the use of the *sPlot* method

for background subtraction by fitting to simulated events, once with only signal candidates, and again to the *sPlot* determined from a mass fit to a sample containing the signal and background in proportions determined from the data.

Assuming no CP violation in decay, we find

$$\phi_s = 0.02 \pm 0.17 \text{(stat)} \pm 0.02 \text{(syst) rad,}$$

where the first uncertainty is statistical and the second is systematic. In a fit to the same data in which we allow for the presence of CP violation in decay, we find

$$\phi_s = 0.02 \pm 0.17 \text{(stat)} \pm 0.02 \text{(syst) rad,}$$

$$|\lambda| = 0.91^{+0.18}_{-0.15} \text{(stat)} \pm 0.02 \text{(syst),}$$

where ϕ_s and $|\lambda|$ have a correlation coefficient of 3%. This measurement is consistent with no CP violation. The decay time distribution and the corresponding fit projection for the case where CP violation in decay is allowed are shown in Fig. 3.
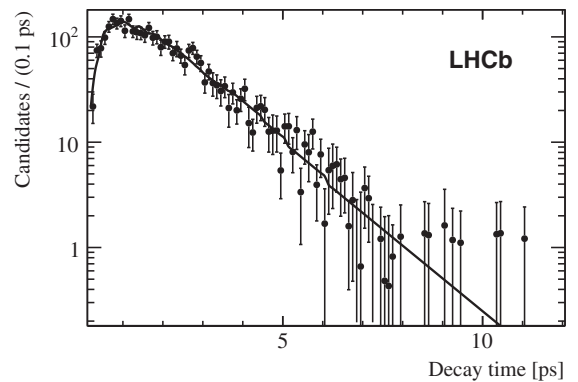
TABLE I.   Summary of systematic uncertainties not already accounted for in the fit, where σ denotes the statistical uncertainty.

Systematic uncertainty	ϕ_s ($\|\lambda\| = 1$)(σ)	$\phi_s(\sigma)$	$\|\lambda\|(\sigma)$
Resolution	± 0.098	± 0.094	± 0.100
Mass	± 0.044	± 0.043	± 0.010
Acceptance (model)	± 0.022	± 0.027	± 0.027
Acceptance (statistical)	± 0.013	± 0.013	± 0.014
Background subtraction	± 0.009	± 0.008	± 0.046
Total	± 0.11	± 0.11	± 0.11

FIG. 3.   Distribution of the decay time for $\bar{B}_s^0 \to D_s^+ D_s^-$ signal decays with background subtracted using the *sPlot* method, along with the fit as described in the text. Discontinuities in the fit line shape are a result of the binned acceptance.

In conclusion, we present the first analysis of the time evolution of flavor-tagged $\bar{B}_s^0 \to D_s^+ D_s^-$ decays. We measure the CP-violating weak phase ϕ_s, allowing for the presence of CP violation in decay, and find that it is consistent with the standard model expectation and with measurements of ϕ_s in other decay modes.

[1] J. Charles *et al.*, Phys. Rev. D **84**, 033005 (2011).
[2] T. Aaltonen *et al.* (CDF Collaboration), Phys. Rev. Lett. **100**, 161802 (2008).
[3] V. M. Abazov *et al.* (D0 Collaboration), Phys. Rev. Lett. **101**, 241801 (2008).
[4] R. Aaij *et al.* (LHCb Collaboration), Phys. Rev. D **87**, 112010 (2013).
[5] R. Aaij *et al.* (LHCb Collaboration), Phys. Lett. B **736**, 186 (2014).
[6] V. M. Abazov *et al.* (D0 Collaboration), Phys. Rev. D **85**, 032006 (2012).
[7] G. Aad *et al.* (ATLAS Collaboration), J. High Energy Phys. 12 (2012) 072.
[8] T. Aaltonen *et al.* (CDF Collaboration), Phys. Rev. Lett. **109**, 171802 (2012).
[9] Y. Amhis *et al.* (Heavy Flavor Averaging Group), arXiv:1207.1158, with updated results and plots available at http://www.slac.stanford.edu/xorg/hfag/.
[10] S. Faller, R. Fleischer, and T. Mannel, Phys. Rev. D **79**, 014005 (2009).
[11] R. Fleischer, Eur. Phys. J. C **51**, 849 (2007).
[12] I. Dunietz, R. Fleischer, and U. Nierste, Phys. Rev. D **63**, 114015 (2001).
[13] A. A. Alves, Jr. *et al.* (LHCb Collaboration), JINST **3**, S08005 (2008).
[14] R. Aaij *et al.*, JINST **8**, P04022 (2013).
[15] V. V. Gligorov and M. Williams, JINST **8**, P02013 (2013).
[16] R. Aaij *et al.* (LHCb Collaboration), Phys. Rev. Lett. **112**, 111802 (2014).
[17] K. A. Olive *et al.* (Particle Data Group), Chin. Phys. C **38**, 090001 (2014).
[18] R. Aaij *et al.* (LHCb Collaboration), Phys. Rev. D **87**, 092007 (2013).
[19] W. D. Hulsbergen, Nucl. Instrum. Methods Phys. Res., Sect. A **552**, 566 (2005).
[20] L. Breiman, J. H. Friedman, R. A. Olshen, and C. J. Stone, *Classification and Regression Trees*, (Wadsworth International Group, Belmont, CA, USA, 1984).
[21] R. E. Schapire and Y. Freund, J. Comput. Syst. Sci. **55**, 119 (1997).
[22] T. Sjöstrand, S. Mrenna, and P. Skands, J. High Energy Phys. 05 (2006) 026; I. Belyaev *et al.*, Nuclear Science Symposium Conference Record (NSS/MIC) IEEE 1155 (2010).
[23] D. J. Lange, Nucl. Instrum. Methods Phys. Res., Sect. A **462**, 152 (2001).
[24] P. Golonka and Z. Was, Eur. Phys. J. C **45**, 97 (2006).
[25] J. Allison *et al.* (Geant4 Collaboration), IEEE Trans. Nucl. Sci. **53**, 270 (2006); S. Agostinelli *et al.* (Geant4 Collaboration), Nucl. Instrum. Methods Phys. Res., Sect. A **506**, 250 (2003); M. Clemencic, G. Corti, S. Easo, C. R. Jones, S. Miglioranzi, M. Pappagallo, and P. Robbe, J. Phys. Conf. Ser. **331**, 032023 (2011).
[26] M. Pivk and F. R. Le Diberder, Nucl. Instrum. Methods Phys. Res., Sect. A **555**, 356 (2005).
[27] Y. Xie, arXiv:0905.0724.
[28] R. Aaij *et al.* (LHCb Collaboration), New J. Phys. **15**, 053021 (2013).
[29] R. Aaij *et al.* (LHCb Collaboration), arXiv:1408.0275 [(to be published)].
[30] R. Aaij *et al.* (LHCb Collaboration), Phys. Lett. B **728**, 607 (2014).
[31] R. Aaij *et al.* (LHCb Collaboration), Eur. Phys. J. C **72**, 2022 (2012).
[32] R. Aaij *et al.* (LHCb Collaboration), arXiv:1407.6127 [(to be published)].

R. Aaij,[41] C. Abellán Beteta,[40] B. Adeva,[37] M. Adinolfi,[46] A. Affolder,[52] Z. Ajaltouni,[5] S. Akar,[6] J. Albrecht,[9] F. Alessio,[38] M. Alexander,[51] S. Ali,[41] G. Alkhazov,[30] P. Alvarez Cartelle,[37] A. A. Alves Jr.,[25,38] S. Amato,[2] S. Amerio,[22] Y. Amhis,[7] L. An,[3] L. Anderlini,[17,a] J. Anderson,[40] R. Andreassen,[57] M. Andreotti,[16,b] J. E. Andrews,[58] R. B. Appleby,[54]

O. Aquines Gutierrez,[10] F. Archilli,[38] A. Artamonov,[35] M. Artuso,[59] E. Aslanides,[6] G. Auriemma,[25,c] M. Baalouch,[5] S. Bachmann,[11] J. J. Back,[48] A. Badalov,[36] C. Baesso,[60] W. Baldini,[16] R. J. Barlow,[54] C. Barschel,[38] S. Barsuk,[7] W. Barter,[47] V. Batozskaya,[28] V. Battista,[39] A. Bay,[39] L. Beaucourt,[4] J. Beddow,[51] F. Bedeschi,[23] I. Bediaga,[1] S. Belogurov,[31] K. Belous,[35] I. Belyaev,[31] E. Ben-Haim,[8] G. Bencivenni,[18] S. Benson,[38] J. Benton,[46] A. Berezhnoy,[32] R. Bernet,[40] M.-O. Bettler,[47] M. van Beuzekom,[41] A. Bien,[11] S. Bifani,[45] T. Bird,[54] A. Bizzeti,[17,d] P. M. Bjørnstad,[54] T. Blake,[48] F. Blanc,[39] J. Blouw,[10] S. Blusk,[59] V. Bocci,[25] A. Bondar,[34] N. Bondar,[30,38] W. Bonivento,[15,38] S. Borghi,[54] A. Borgia,[59] M. Borsato,[7] T. J. V. Bowcock,[52] E. Bowen,[40] C. Bozzi,[16] T. Brambach,[9] D. Brett,[54] M. Britsch,[10] T. Britton,[59] J. Brodzicka,[54] N. H. Brook,[46] H. Brown,[52] A. Bursche,[40] G. Busetto,[22,e] J. Buytaert,[38] S. Cadeddu,[15] R. Calabrese,[16,b] M. Calvi,[20,f] M. Calvo Gomez,[36,g] P. Campana,[18] D. Campora Perez,[38] A. Carbone,[14,h] G. Carboni,[24,i] R. Cardinale,[19,38,j] A. Cardini,[15] L. Carson,[50] K. Carvalho Akiba,[2] G. Casse,[52] L. Cassina,[20] L. Castillo Garcia,[38] M. Cattaneo,[38] Ch. Cauet,[9] R. Cenci,[58] M. Charles,[8] Ph. Charpentier,[38] M. Chefdeville,[4] S. Chen,[54] S.-F. Cheung,[55] N. Chiapolini,[40] M. Chrzaszcz,[40,26] X. Cid Vidal,[38] G. Ciezarek,[53] P. E. L. Clarke,[50] M. Clemencic,[38] H. V. Cliff,[47] J. Closier,[38] V. Coco,[38] J. Cogan,[6] E. Cogneras,[5] V. Cogoni,[15] L. Cojocariu,[29] P. Collins,[38] A. Comerma-Montells,[11] A. Contu,[15,38] A. Cook,[46] M. Coombes,[46] S. Coquereau,[8] G. Corti,[38] M. Corvo,[16,b] I. Counts,[56] B. Couturier,[38] G. A. Cowan,[50] D. C. Craik,[48] M. Cruz Torres,[60] S. Cunliffe,[53] R. Currie,[50] C. D'Ambrosio,[38] J. Dalseno,[46] P. David,[8] P. N. Y. David,[41] A. Davis,[57] K. De Bruyn,[41] S. De Capua,[54] M. De Cian,[11] J. M. De Miranda,[1] L. De Paula,[2] W. De Silva,[57] P. De Simone,[18] D. Decamp,[4] M. Deckenhoff,[9] L. Del Buono,[8] N. Déléage,[4] D. Derkach,[55] O. Deschamps,[5] F. Dettori,[38] A. Di Canto,[38] H. Dijkstra,[38] S. Donleavy,[52] F. Dordei,[11] M. Dorigo,[39] A. Dosil Suárez,[37] D. Dossett,[48] A. Dovbnya,[43] K. Dreimanis,[52] G. Dujany,[54] F. Dupertuis,[39] P. Durante,[38] R. Dzhelyadin,[35] A. Dziurda,[26] A. Dzyuba,[30] S. Easo,[49,38] U. Egede,[53] V. Egorychev,[31] S. Eidelman,[34] S. Eisenhardt,[50] U. Eitschberger,[9] R. Ekelhof,[9] L. Eklund,[51] I. El Rifai,[5] E. Elena,[40] Ch. Elsasser,[40] S. Ely,[59] S. Esen,[11] H.-M. Evans,[47] T. Evans,[55] A. Falabella,[14] C. Färber,[11] C. Farinelli,[41] N. Farley,[45] S. Farry,[52] RF Fay,[52] D. Ferguson,[50] V. Fernandez Albor,[37] F. Ferreira Rodrigues,[1] M. Ferro-Luzzi,[38] S. Filippov,[33] M. Fiore,[16,b] M. Fiorini,[16,b] M. Firlej,[27] C. Fitzpatrick,[39] T. Fiutowski,[27] P. Fol,[53] M. Fontana,[10] F. Fontanelli,[19,j] R. Forty,[38] O. Francisco,[2] M. Frank,[38] C. Frei,[38] M. Frosini,[17,a] J. Fu,[21,38] E. Furfaro,[24,i] A. Gallas Torreira,[37] D. Galli,[14,h] S. Gallorini,[22,38] S. Gambetta,[19,j] M. Gandelman,[2] P. Gandini,[59] Y. Gao,[3] J. García Pardiñas,[37] J. Garofoli,[59] J. Garra Tico,[47] L. Garrido,[36] C. Gaspar,[38] R. Gauld,[55] L. Gavardi,[9] G. Gavrilov,[30] A. Geraci,[21,k] E. Gersabeck,[11] M. Gersabeck,[54] T. Gershon,[48] Ph. Ghez,[4] A. Gianelle,[22] S. Gianì,[39] V. Gibson,[47] L. Giubega,[29] V. V. Gligorov,[38] C. Göbel,[60] D. Golubkov,[31] A. Golutvin,[53,31,38] A. Gomes,[1,l] C. Gotti,[20] M. Grabalosa Gándara,[5] R. Graciani Diaz,[36] L. A. Granado Cardoso,[38] E. Graugés,[36] G. Graziani,[17] A. Grecu,[29] E. Greening,[55] S. Gregson,[47] P. Griffith,[45] L. Grillo,[11] O. Grünberg,[62] B. Gui,[59] E. Gushchin,[33] Yu. Guz,[35,38] T. Gys,[38] C. Hadjivasiliou,[59] G. Haefeli,[39] C. Haen,[38] S. C. Haines,[47] S. Hall,[53] B. Hamilton,[58] T. Hampson,[46] X. Han,[11] S. Hansmann-Menzemer,[11] N. Harnew,[55] S. T. Harnew,[46] J. Harrison,[54] J. He,[38] T. Head,[38] V. Heijne,[41] K. Hennessy,[52] P. Henrard,[5] L. Henry,[8] J. A. Hernando Morata,[37] E. van Herwijnen,[38] M. Heß,[62] A. Hicheur,[2] D. Hill,[55] M. Hoballah,[5] C. Hombach,[54] W. Hulsbergen,[41] P. Hunt,[55] N. Hussain,[55] D. Hutchcroft,[52] D. Hynds,[51] M. Idzik,[27] P. Ilten,[56] R. Jacobsson,[38] A. Jaeger,[11] J. Jalocha,[55] E. Jans,[41] P. Jaton,[39] A. Jawahery,[58] F. Jing,[3] M. John,[55] D. Johnson,[38] C. R. Jones,[47] C. Joram,[38] B. Jost,[38] N. Jurik,[59] M. Kaballo,[9] S. Kandybei,[43] W. Kanso,[6] M. Karacson,[38] T. M. Karbach,[38] S. Karodia,[51] M. Kelsey,[59] I. R. Kenyon,[45] T. Ketel,[42] B. Khanji,[20,38] C. Khurewathanakul,[39] S. Klaver,[54] K. Klimaszewski,[28] O. Kochebina,[7] M. Kolpin,[11] I. Komarov,[39] R. F. Koopman,[42] P. Koppenburg,[41,38] M. Korolev,[32] A. Kozlinskiy,[41] L. Kravchuk,[33] K. Kreplin,[11] M. Kreps,[48] G. Krocker,[11] P. Krokovny,[34] F. Kruse,[9] W. Kucewicz,[26,m] M. Kucharczyk,[20,26,f] V. Kudryavtsev,[34] K. Kurek,[28] T. Kvaratskheliya,[31] V. N. La Thi,[39] D. Lacarrere,[38] G. Lafferty,[54] A. Lai,[15] D. Lambert,[50] R. W. Lambert,[42] G. Lanfranchi,[18] C. Langenbruch,[48] B. Langhans,[38] T. Latham,[48] C. Lazzeroni,[45] R. Le Gac,[6] J. van Leerdam,[41] J.-P. Lees,[4] R. Lefèvre,[5] A. Leflat,[32] J. Lefrançois,[7] S. Leo,[23] O. Leroy,[6] T. Lesiak,[26] B. Leverington,[11] Y. Li,[3] T. Likhomanenko,[63] M. Liles,[52] R. Lindner,[38] C. Linn,[38] F. Lionetto,[40] B. Liu,[15] S. Lohn,[38] I. Longstaff,[51] J. H. Lopes,[2] N. Lopez-March,[39] P. Lowdon,[40] D. Lucchesi,[22,e] H. Luo,[50] A. Lupato,[22] E. Luppi,[16,b] O. Lupton,[55] F. Machefert,[7] I. V. Machikhiliyan,[31] F. Maciuc,[29] O. Maev,[30] S. Malde,[55] A. Malinin,[63] G. Manca,[15,n] G. Mancinelli,[6] A. Mapelli,[38] J. Maratas,[5] J. F. Marchand,[4] U. Marconi,[14] C. Marin Benito,[36] P. Marino,[23,o] R. Märki,[39] J. Marks,[11] G. Martellotti,[25] A. Martín Sánchez,[7] M. Martinelli,[39] D. Martinez Santos,[42,38] F. Martinez Vidal,[64] D. Martins Tostes,[2] A. Massafferri,[1] R. Matev,[38] Z. Mathe,[38] C. Matteuzzi,[20] A. Mazurov,[45] M. McCann,[53] J. McCarthy,[45] A. McNab,[54] R. McNulty,[12] B. McSkelly,[52] B. Meadows,[57] F. Meier,[9] M. Meissner,[11] M. Merk,[41] D. A. Milanes,[8] M.-N. Minard,[4] N. Moggi,[14] J. Molina Rodriguez,[60] S. Monteil,[5] M. Morandin,[22] P. Morawski,[27] A. Mordà,[6] M. J. Morello,[23,o] J. Moron,[27]

A.-B. Morris,[50] R. Mountain,[59] F. Muheim,[50] K. Müller,[40] M. Mussini,[14] B. Muster,[39] P. Naik,[46] T. Nakada,[39]
R. Nandakumar,[49] I. Nasteva,[2] M. Needham,[50] N. Neri,[21] S. Neubert,[38] N. Neufeld,[38] M. Neuner,[11] A. D. Nguyen,[39]
T. D. Nguyen,[39] C. Nguyen-Mau,[39,p] M. Nicol,[7] V. Niess,[5] R. Niet,[9] N. Nikitin,[32] T. Nikodem,[11] A. Novoselov,[35]
D. P. O'Hanlon,[48] A. Oblakowska-Mucha,[27,38] V. Obraztsov,[35] S. Oggero,[41] S. Ogilvy,[51] O. Okhrimenko,[44] R. Oldeman,[15,n]
G. Onderwater,[65] M. Orlandea,[29] J. M. Otalora Goicochea,[2] A. Otto,[38] P. Owen,[53] A. Oyanguren,[64] B. K. Pal,[59]
A. Palano,[13,q] F. Palombo,[21,r] M. Palutan,[18] J. Panman,[38] A. Papanestis,[49,38] M. Pappagallo,[51] L. L. Pappalardo,[16,b]
C. Parkes,[54] C. J. Parkinson,[9,45] G. Passaleva,[17] G. D. Patel,[52] M. Patel,[53] C. Patrignani,[19,j] A. Pazos Alvarez,[37] A. Pearce,[54]
A. Pellegrino,[41] M. Pepe Altarelli,[38] S. Perazzini,[14,h] E. Perez Trigo,[37] P. Perret,[5] M. Perrin-Terrin,[6] L. Pescatore,[45]
E. Pesen,[66] K. Petridis,[53] A. Petrolini,[19,j] E. Picatoste Olloqui,[36] B. Pietrzyk,[4] T. Pilař,[48] D. Pinci,[25] A. Pistone,[19] S. Playfer,[50]
M. Plo Casasus,[37] F. Polci,[8] A. Poluektov,[48,34] E. Polycarpo,[2] A. Popov,[35] D. Popov,[10] B. Popovici,[29] C. Potterat,[2] E. Price,[46]
J. D. Price,[52] J. Prisciandaro,[39] A. Pritchard,[52] C. Prouve,[46] V. Pugatch,[44] A. Puig Navarro,[39] G. Punzi,[23,s] W. Qian,[4]
B. Rachwal,[26] J. H. Rademacker,[46] B. Rakotomiaramanana,[39] M. Rama,[18] M. S. Rangel,[2] I. Raniuk,[43] N. Rauschmayr,[38]
G. Raven,[42] F. Redi,[53] S. Reichert,[54] M. M. Reid,[48] A. C. dos Reis,[1] S. Ricciardi,[49] S. Richards,[46] M. Rihl,[38] K. Rinnert,[52]
V. Rives Molina,[36] P. Robbe,[7] A. B. Rodrigues,[1] E. Rodrigues,[54] P. Rodriguez Perez,[54] S. Roiser,[38] V. Romanovsky,[35]
A. Romero Vidal,[37] M. Rotondo,[22] J. Rouvinet,[39] T. Ruf,[38] H. Ruiz,[36] P. Ruiz Valls,[64] J. J. Saborido Silva,[37] N. Sagidova,[30]
P. Sail,[51] B. Saitta,[15,n] V. Salustino Guimaraes,[2] C. Sanchez Mayordomo,[64] B. Sanmartin Sedes,[37] R. Santacesaria,[25]
C. Santamarina Rios,[37] E. Santovetti,[24,i] A. Sarti,[18,t] C. Satriano,[25,c] A. Satta,[24] D. M. Saunders,[46] M. Savrie,[16,b]
D. Savrina,[31,32] M. Schiller,[42] H. Schindler,[38] M. Schlupp,[9] M. Schmelling,[10] B. Schmidt,[38] O. Schneider,[39] A. Schopper,[38]
M.-H. Schune,[7] R. Schwemmer,[38] B. Sciascia,[18] A. Sciubba,[25] M. Seco,[37] A. Semennikov,[31] I. Sepp,[53] N. Serra,[40]
J. Serrano,[6] L. Sestini,[22] P. Seyfert,[11] M. Shapkin,[35] I. Shapoval,[16,43,b] Y. Shcheglov,[30] T. Shears,[52] L. Shekhtman,[34]
V. Shevchenko,[63] A. Shires,[9] R. Silva Coutinho,[48] G. Simi,[22] M. Sirendi,[47] N. Skidmore,[46] I. Skillicorn,[51] T. Skwarnicki,[59]
N. A. Smith,[52] E. Smith,[55,49] E. Smith,[53] J. Smith,[47] M. Smith,[54] H. Snoek,[41] M. D. Sokoloff,[57] F. J. P. Soler,[51] F. Soomro,[39]
D. Souza,[46] B. Souza De Paula,[2] B. Spaan,[9] P. Spradlin,[51] S. Sridharan,[38] F. Stagni,[38] M. Stahl,[11] S. Stahl,[11] O. Steinkamp,[40]
O. Stenyakin,[35] S. Stevenson,[55] S. Stoica,[29] S. Stone,[59] B. Storaci,[40] S. Stracka,[23] M. Straticiuc,[29] U. Straumann,[40]
R. Stroili,[22] V. K. Subbiah,[38] L. Sun,[57] W. Sutcliffe,[53] K. Swientek,[27] S. Swientek,[9] V. Syropoulos,[42] M. Szczekowski,[28]
P. Szczypka,[39,38] D. Szilard,[2] T. Szumlak,[27] S. T'Jampens,[4] M. Teklishyn,[7] G. Tellarini,[16,b] F. Teubert,[38] C. Thomas,[55]
E. Thomas,[38] J. van Tilburg,[41] V. Tisserand,[4] M. Tobin,[39] J. Todd,[57] S. Tolk,[42] L. Tomassetti,[16,b] D. Tonelli,[38]
S. Topp-Joergensen,[55] N. Torr,[55] E. Tournefier,[4] S. Tourneur,[39] M. T. Tran,[39] M. Tresch,[40] A. Tsaregorodtsev,[6] P. Tsopelas,[41]
N. Tuning,[41] M. Ubeda Garcia,[38] A. Ukleja,[28] A. Ustyuzhanin,[63] U. Uwer,[11] C. Vacca,[15] V. Vagnoni,[14] G. Valenti,[14]
A. Vallier,[7] R. Vazquez Gomez,[18] P. Vazquez Regueiro,[37] C. Vázquez Sierra,[37] S. Vecchi,[16] J. J. Velthuis,[46] M. Veltri,[17,u]
G. Veneziano,[39] M. Vesterinen,[11] B. Viaud,[7] D. Vieira,[2] M. Vieites Diaz,[37] X. Vilasis-Cardona,[36,g] A. Vollhardt,[40]
D. Volyanskyy,[10] D. Voong,[46] A. Vorobyev,[30] V. Vorobyev,[34] C. Voß,[62] H. Voss,[10] J. A. de Vries,[41] R. Waldi,[62] C. Wallace,[48]
R. Wallace,[12] J. Walsh,[23] S. Wandernoth,[11] J. Wang,[59] D. R. Ward,[47] N. K. Watson,[45] D. Websdale,[53] M. Whitehead,[48]
J. Wicht,[38] D. Wiedner,[11] G. Wilkinson,[55,38] M. P. Williams,[45] M. Williams,[56] H. W. Wilschut,[65] F. F. Wilson,[49]
J. Wimberley,[58] J. Wishahi,[9] W. Wislicki,[28] M. Witek,[26] G. Wormser,[7] S. A. Wotton,[47] S. Wright,[47] K. Wyllie,[38] Y. Xie,[61]
Z. Xing,[59] Z. Xu,[39] Z. Yang,[3] X. Yuan,[3] O. Yushchenko,[35] M. Zangoli,[14] M. Zavertyaev,[10,v] L. Zhang,[59] W. C. Zhang,[12]
Y. Zhang,[3] A. Zhelezov,[11] A. Zhokhov[31] and L. Zhong[3]

(LHCb Collaboration)

[1]Centro Brasileiro de Pesquisas Físicas (CBPF), Rio de Janeiro, Brazil
[2]Universidade Federal do Rio de Janeiro (UFRJ), Rio de Janeiro, Brazil
[3]Center for High Energy Physics, Tsinghua University, Beijing, China
[4]LAPP, Université de Savoie, CNRS/IN2P3, Annecy-Le-Vieux, France
[5]Clermont Université, Université Blaise Pascal, CNRS/IN2P3, LPC, Clermont-Ferrand, France
[6]CPPM, Aix-Marseille Université, CNRS/IN2P3, Marseille, France
[7]LAL, Université Paris-Sud, CNRS/IN2P3, Orsay, France
[8]LPNHE, Université Pierre et Marie Curie, Université Paris Diderot, CNRS/IN2P3, Paris, France
[9]Fakultät Physik, Technische Universität Dortmund, Dortmund, Germany
[10]Max-Planck-Institut für Kernphysik (MPIK), Heidelberg, Germany
[11]Physikalisches Institut, Ruprecht-Karls-Universität Heidelberg, Heidelberg, Germany

[12]School of Physics, University College Dublin, Dublin, Ireland
[13]Sezione INFN di Bari, Bari, Italy
[14]Sezione INFN di Bologna, Bologna, Italy
[15]Sezione INFN di Cagliari, Cagliari, Italy
[16]Sezione INFN di Ferrara, Ferrara, Italy
[17]Sezione INFN di Firenze, Firenze, Italy
[18]Laboratori Nazionali dell'INFN di Frascati, Frascati, Italy
[19]Sezione INFN di Genova, Genova, Italy
[20]Sezione INFN di Milano Bicocca, Milano, Italy
[21]Sezione INFN di Milano, Milano, Italy
[22]Sezione INFN di Padova, Padova, Italy
[23]Sezione INFN di Pisa, Pisa, Italy
[24]Sezione INFN di Roma Tor Vergata, Roma, Italy
[25]Sezione INFN di Roma La Sapienza, Roma, Italy
[26]Henryk Niewodniczanski Institute of Nuclear Physics Polish Academy of Sciences, Kraków, Poland
[27]AGH - University of Science and Technology, Faculty of Physics and Applied Computer Science,
Kraków, Poland
[28]National Center for Nuclear Research (NCBJ), Warsaw, Poland
[29]Horia Hulubei National Institute of Physics and Nuclear Engineering, Bucharest-Magurele, Romania
[30]Petersburg Nuclear Physics Institute (PNPI), Gatchina, Russia
[31]Institute of Theoretical and Experimental Physics (ITEP), Moscow, Russia
[32]Institute of Nuclear Physics, Moscow State University (SINP MSU), Moscow, Russia
[33]Institute for Nuclear Research of the Russian Academy of Sciences (INR RAN), Moscow, Russia
[34]Budker Institute of Nuclear Physics (SB RAS) and Novosibirsk State University, Novosibirsk, Russia
[35]Institute for High Energy Physics (IHEP), Protvino, Russia
[36]Universitat de Barcelona, Barcelona, Spain
[37]Universidad de Santiago de Compostela, Santiago de Compostela, Spain
[38]European Organization for Nuclear Research (CERN), Geneva, Switzerland
[39]Ecole Polytechnique Fédérale de Lausanne (EPFL), Lausanne, Switzerland
[40]Physik-Institut, Universität Zürich, Zürich, Switzerland
[41]Nikhef National Institute for Subatomic Physics, Amsterdam, The Netherlands
[42]Nikhef National Institute for Subatomic Physics and VU University Amsterdam,
Amsterdam, The Netherlands
[43]NSC Kharkiv Institute of Physics and Technology (NSC KIPT), Kharkiv, Ukraine
[44]Institute for Nuclear Research of the National Academy of Sciences (KINR), Kyiv, Ukraine
[45]University of Birmingham, Birmingham, United Kingdom
[46]H.H. Wills Physics Laboratory, University of Bristol, Bristol, United Kingdom
[47]Cavendish Laboratory, University of Cambridge, Cambridge, United Kingdom
[48]Department of Physics, University of Warwick, Coventry, United Kingdom
[49]STFC Rutherford Appleton Laboratory, Didcot, United Kingdom
[50]School of Physics and Astronomy, University of Edinburgh, Edinburgh, United Kingdom
[51]School of Physics and Astronomy, University of Glasgow, Glasgow, United Kingdom
[52]Oliver Lodge Laboratory, University of Liverpool, Liverpool, United Kingdom
[53]Imperial College London, London, United Kingdom
[54]School of Physics and Astronomy, University of Manchester, Manchester, United Kingdom
[55]Department of Physics, University of Oxford, Oxford, United Kingdom
[56]Massachusetts Institute of Technology, Cambridge, Massachusetts, USA
[57]University of Cincinnati, Cincinnati, Ohio, USA
[58]University of Maryland, College Park, Maryland, USA
[59]Syracuse University, Syracuse, New York, USA
[60]Pontifícia Universidade Católica do Rio de Janeiro (PUC-Rio), Rio de Janeiro, Brazil
(associated with Universidade Federal do Rio de Janeiro (UFRJ), Rio de Janeiro, Brazil)
[61]Institute of Particle Physics, Central China Normal University, Wuhan, Hubei, China
(associated with Center for High Energy Physics, Tsinghua University, Beijing, China)
[62]Institut für Physik, Universität Rostock, Rostock, Germany (associated with Physikalisches Institut,
Ruprecht-Karls-Universität Heidelberg, Heidelberg, Germany)
[63]National Research Centre Kurchatov Institute, Moscow, Russia
(associated with Institute of Theoretical and Experimental Physics (ITEP), Moscow, Russia)
[64]Instituto de Fisica Corpuscular (IFIC), Universitat de Valencia-CSIC, Valencia, Spain
(associated with Universitat de Barcelona, Barcelona, Spain)

[65]*KVI - University of Groningen, Groningen, The Netherlands*
(associated with Nikhef National Institute for Subatomic Physics, Amsterdam, The Netherlands)
[66]*Celal Bayar University, Manisa, Turkey*
(associated with European Organization for Nuclear Research (CERN), Geneva, Switzerland)

[a]Also at Università di Firenze, Firenze, Italy.

[b]Also at Università di Ferrara, Ferrara, Italy.

[c]Also at Università della Basilicata, Potenza, Italy.

[d]Also at Università di Modena e Reggio Emilia, Modena, Italy.

[e]Also at Università di Padova, Padova, Italy.

[f]Also at Università di Milano Bicocca, Milano, Italy.

[g]Also at LIFAELS, La Salle, Universitat Ramon Llull, Barcelona, Spain.

[h]Also at Università di Bologna, Bologna, Italy.

[i]Also at Università di Roma Tor Vergata, Roma, Italy.

[j]Also at Università di Genova, Genova, Italy.

[k]Also at Politecnico di Milano, Milano, Italy.

[l]Also at Universidade Federal do Triângulo Mineiro (UFTM), Uberaba-MG, Brazil.

[m]Also at AGH - University of Science and Technology, Faculty of Computer Science, Electronics and Telecommunications, Kraków, Poland.

[n]Also at Università di Cagliari, Cagliari, Italy.

[o]Also at Scuola Normale Superiore, Pisa, Italy.

[p]Also at Hanoi University of Science, Hanoi, Vietnam.

[q]Also at Università di Bari, Bari, Italy.

[r]Also at Università degli Studi di Milano, Milano, Italy.

[s]Also at Università di Pisa, Pisa, Italy.

[t]Also at Università di Roma La Sapienza, Roma, Italy.

[u]Also at Università di Urbino, Urbino, Italy.

[v]Also at P.N. Lebedev Physical Institute, Russian Academy of Science (LPI RAS), Moscow, Russia.